JACS
JOURNAL OF THE AMERICAN CHEMICAL SOCIETY
Cite This: J. Am. Chem. Soc. XXXX, XXX, XXX−XXX
Communication
pubs.acs.org/JACS

Hydronium-Induced Switching between CO_2 Electroreduction Pathways

Ali Seifitokaldani,[†,⊥] Christine M. Gabardo,[‡,⊥] Thomas Burdyny,[‡] Cao-Thang Dinh,[†] Jonathan P. Edwards,[‡] Md Golam Kibria,[†] Oleksandr S. Bushuyev,[†,§] Shana O. Kelley,[§,∥] David Sinton,[‡] and Edward H. Sargent*[,†]

[†]Department of Electrical and Computer Engineering, University of Toronto, 35 St. George Street, Toronto, Ontario M5S 1A4, Canada

[‡]Department of Mechanical and Industrial Engineering, University of Toronto, 5 King's College Road, Toronto, Ontario M5S 3G8, Canada

[§]Department of Chemistry, University of Toronto, 80 St. George Street, Toronto, Ontario M5S 3G4, Canada

[∥]Department of Pharmaceutical Sciences, University of Toronto, Leslie Dan Faculty of Pharmacy, 144 College Street, Toronto, Ontario M5S 3M2, Canada

Supporting Information

ABSTRACT: Over a broad range of operating conditions, many CO_2 electroreduction catalysts can maintain selectivity toward certain reduction products, leading to materials and surfaces being categorized according to their products; here we ask, is product selectivity truly a property of the catalyst? Silver is among the best electrocatalysts for CO in aqueous electrolytes, where it reaches near-unity selectivity. We consider the hydrogenations of the oxygen and carbon atoms via the two proton-coupled-electron-transfer processes as chief determinants of product selectivity; and find using density functional theory (DFT) that the hydronium (H_3O^+) intermediate plays a key role in the first oxygen hydrogenation step and lowers the activation energy barrier for CO formation. When this hydronium influence is removed, the activation energy barrier for oxygen hydrogenation increases significantly, and the barrier for carbon hydrogenation is reduced. These effects make the formate reaction pathway more favorable than CO. Experimentally, we then carry out CO_2 reduction in highly concentrated potassium hydroxide (KOH), limiting the hydronium concentration in the aqueous electrolyte. The product selectivity of a silver catalyst switches from entirely CO under neutral conditions to over 50% formate in the alkaline environment. The simulated and experimentally observed selectivity shift provides new insights into the role of hydronium on CO_2 electroreduction processes and the ability for electrolyte manipulation to directly influence transition state (TS) kinetics, altering favored CO_2 reaction pathways. We argue that selectivity should be considered less of an intrinsic catalyst property, and rather a combined product of the catalyst and reaction environment.

The electrocatalytic CO_2 reduction reaction (CO_2RR) provides a means to upgrade a liability into chemically stored energy. CO_2 can be transformed into a variety of energy-dense carbon-based products, making it a versatile chemical feedstock.[1] Of metal-based catalysts studied for CO_2RR, *p*-block metals, such as Pb, Sn, Bi, and In, primarily produce formate;[2] and some *d*-block metals, such as Ag and Au, are the most selective catalysts for CO.[3] Copper remains the only metal that produces significant multicarbon hydrocarbons and multicarbon oxygenates.[4] Categorizing catalysts by their primary observed products is helpful, but reaction pathways are a combined effect of a catalyst's surface structure and interactions with the surrounding reaction environment. This leads to the question, starting from the same metallic surface can we impose different aqueous conditions to change the observed CO_2 reaction pathways behavior and lead to different products? To investigate these questions we examined CO_2 reduction on a silver catalyst.

Silver is considered the most promising catalyst for CO production due to its high selectivity, activity, and lower price compared to the other noble metal catalysts.[5] Silver-based catalysts have been extensively used in experimental CO_2RR studies;[6] yet the underlying reaction mechanism remains incompletely understood. Computational approaches are often curtailed by the complexity of the electrochemical interface including ions, solvent, interfacial charge, and potential. Nevertheless, several computational studies,[7] have shown that considering explicit water as the main solvent in aqueous electrolytes provides a more realistic picture of the reaction environment. For silver catalysts, prior computational studies[7d,8] investigated the CO_2 reduction to CO, but did not examine the competing reduction reaction to formate, which may be because experimental studies generally report high selectivity to CO.[9]

Here we investigate the activation energy barriers for the two CO_2RR products on silver in aqueous electrolytes. We focus on the TS of the first hydrogenation step (i.e., the rate-determining step) toward the production of both CO (eq 1) and formate (eq 3) and include explicit water in our computations.

Received: December 21, 2017
Published: March 5, 2018

DOI: 10.1021/jacs.7b13542
J. Am. Chem. Soc. XXXX, XXX, XXX−XXX

In the first CO_2RR step, the oxygen hydrogenation pathway (with carboxyl intermediate: COOH) will lead to the production of CO (eq 2) and the carbon hydrogenation pathway (with formate intermediate: CHOO) will lead to the production of formate (eq 4). In all these equations, an asterisk (*) demonstrates the catalyst active site.

$$CO_2 + (H^+ + e^-) + * \rightarrow *COOH \quad (1)$$

$$*COOH + (H^+ + e^-) \rightarrow * + CO + H_2O \quad (2)$$

$$CO_2 + (H^+ + e^-) + * \rightarrow *CHOO \quad (3)$$

$$*CHOO + (H^+ + e^-) \rightarrow * + CHOOH \quad (4)$$

Both oxygen and carbon hydrogenations involve one proton-coupled-electron-transfer process. We took the view that understanding the role of hydronium on the O−H and C−H bond formation steps for the Ag electrode is critical for providing significant insights into the CO_2RR mechanism toward the production of either CO or formate. Further, a better understanding of how the local reaction environment can impact the kinetics of the TS may provide experimental strategies to improve, or change completely, the selectivity of other reactions.

We performed DFT simulations to determine the potential-dependent reaction free energies and activation energy barriers for the two reaction pathways of CO_2RR on silver. We considered (111), (100), and (211) facets of silver in our computational studies. All barrier calculations are performed using the climbing image nudged elastic band method (CI-NEB)[10] with 4 images. We considered an explicit water molecule to assist the hydrogenation step. For the *COOH intermediate, we considered two trans (with H closer to the surface) and cis (with H on top of the oxygen) configurations. Similar to previous studies on copper,[11] we determined the activation energy barrier for hydrogenation reactions. Further computational details are given in the Supporting Information.

To find the minimum activation energy barrier in our simulations, we considered the possible involvement of a single-water molecule in the first hydrogenation step. As previously described in detail,[11] two possible modes of water assistance are studied: (i) a solvated mode (Figure S1-a), in which the hydrogenation step is facilitated by a nearby water molecule, but eventually the surface proton directly combines with the adsorbed CO_2 molecule, and (ii) a H-shuttling mode (Figure S1-b), in which the surface proton combines with the water molecule, and the water molecule donates another proton to the CO_2 molecule. We observed that in both modes, the hydronium (H_3O^+) intermediate will be created from the explicit water molecule.

Figure 1 shows the activation energy barriers for both CO and formate pathways with an explicit water molecule on Ag(111) surface (similar results for Ag(100) and Ag(211) are shown in Figures S2 and S3). Both solvated water and H-shuttling mechanisms significantly reduced the activation energy barrier for the O−H bond formation, leading to CO production (E^0_{act} = 0.65 eV). In both mechanisms, the polar O−H bond formation is stabilized through hydronium. In most of the calculations, the H-shuttling mechanism in a trans configuration showed smaller activation energy barriers for hydrogenation as compared to the solvated mechanism and the cis configurations (for comparison of the two approaches, see Table S1). The minimum activation energy provided by H-shuttling mechanism in the trans configuration for Ag(111) is plotted in Figure 1. For the less polar C−H bond formation in the formate pathway, hydronium-assisted hydrogenation shows a higher activation energy barrier than CO (E^0_{act} = 1.197 eV), making formate production less favorable.

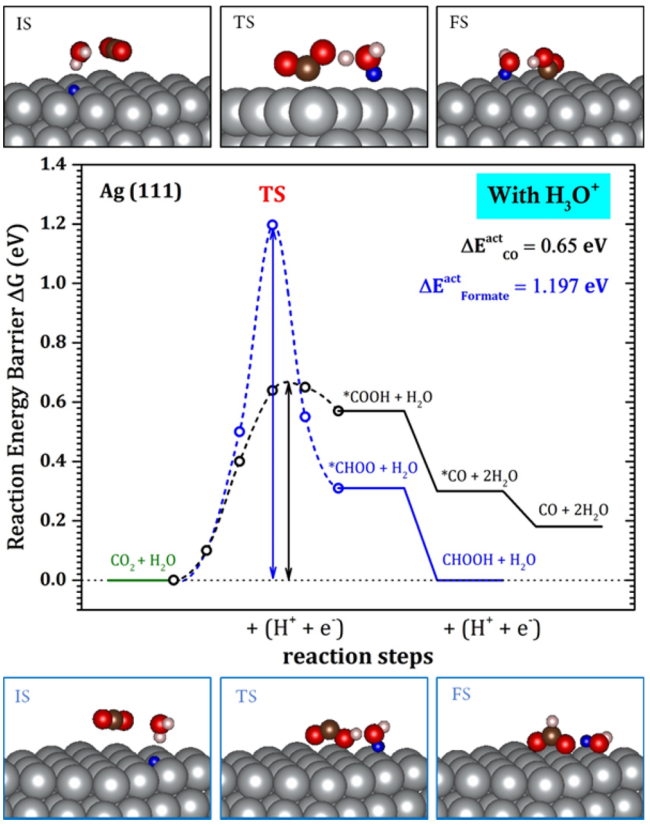

Figure 1. Activation energy barriers at equilibrium potential for CO (black) and formate (blue) pathways with hydronium on Ag(111). The top and bottom panels depict three initial (left), transition (middle), and final (right) states for the CO pathway and formate pathway, respectively. The brown and red spheres represent carbon and oxygen, respectively, whereas white and blue both represent hydrogen atom.

Next, we calculated the activation energy barriers through a direct hydrogenation mechanism, where water does not assist in the hydrogenation process (Figure 2). Without hydronium present, the COOH intermediate with cis configuration possesses a slightly lower activation energy barrier compared to the trans configuration (Table S1). As shown in Figure 2, the overall activation energy barrier for the rate-determining COOH intermediate, however, is significantly higher (E^0_{act} = 2.87 eV) when there is no hydronium assistance to stabilize the O−H bond formation. On the other hand, the activation energy barrier of the CHOO intermediate leading to formate is seen to decrease (E^0_{act} = 0.67eV). Without hydronium assistance, we conclude that formate is energetically favored over CO formation (Table S2).

It is evident that the activation energies for CO and formate were very different with (Figure 1) and without (Figure 2) the hydronium intermediate present. On Ag(111), with hydronium, the CO pathway has a lower activation energy barrier (0.65 eV) compared to the formate pathway (1.197 eV). Interestingly, in the absence of the hydronium-assisted mechanism, there exists a large activation energy barrier for O−H bond formation (2.87 eV for COOH intermediate) and a

DOI: 10.1021/jacs.7b13542
J. Am. Chem. Soc. XXXX, XXX, XXX−XXX

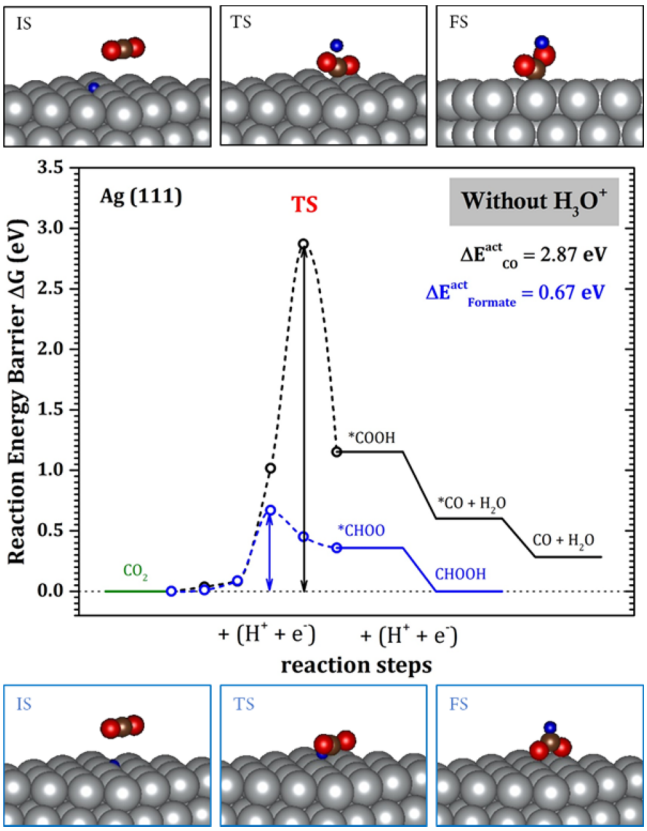

Figure 2. Activation energy barriers at equilibrium potential for CO (black) and formate (blue) pathways without hydronium on Ag(111). The top and bottom panels depict three initial (left), transition (middle), and final (right) states for the CO pathway and formate pathway, respectively. The brown, red, and blue spheres represent carbon, oxygen, and hydrogen, respectively.

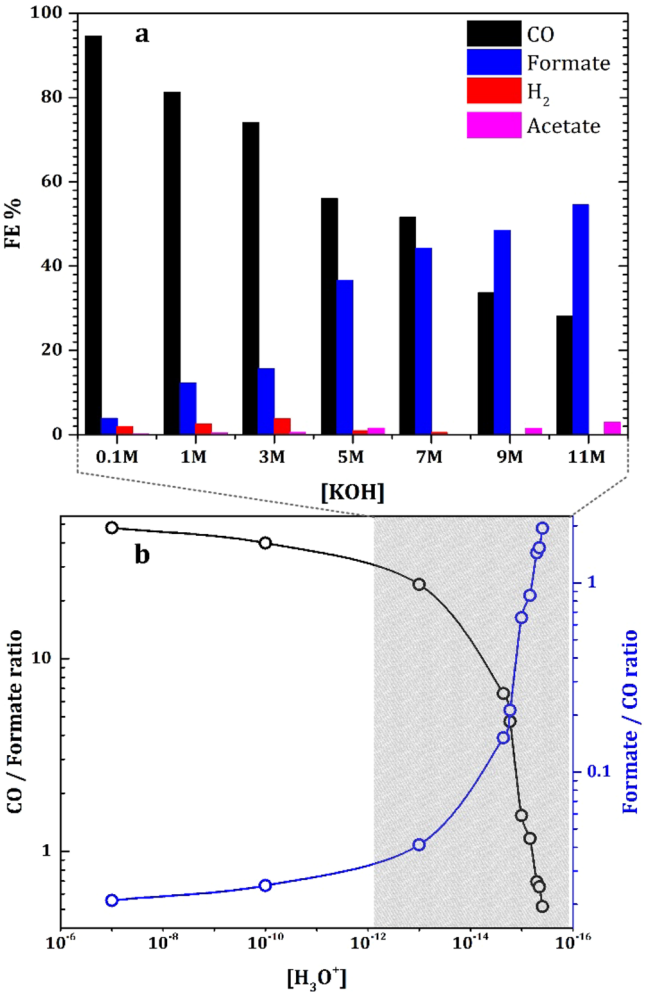

Figure 3. Experimental study of effect of hydronium concentration on CO_2RR product selectivity. (a) FE for the CO_2RR products at different KOH concentrations (300 mA/cm^2). (b) The CO:formate ratio (left *y*-axis) and its inverse (right *y*-axis) at different hydronium concentrations.

much smaller barrier for the C−H bond formation (0.67 eV for CHOO intermediate).

To experimentally confirm the theoretically predicted hydronium hypothesis for product selectivity, we tuned the hydronium concentration in aqueous electrolytes using a strong base, KOH, to destabilize hydronium ions. CO_2RR was conducted in a flow cell configuration using a silver catalyst deposited on a gas diffusion electrode in order to allow for highly alkaline electrolyte conditions (further experimental details provided in the Supporting Information). As the hydroxide concentration increased, and consequently hydronium concentration decreased, the production of CO was suppressed and the Faradaic efficiency (FE) for formate increased (Figure 3). The CO:formate ratio decreased by 2 orders of magnitude from 48 at pH 7 to 0.69 at pH > 15. To eliminate the increase in potassium ions as the source of the product selectivity switching, KI was tested as the electrolyte at various concentrations (Figure S5). The CO:formate ratios did not vary significantly over the range of KI tested, supporting the hypothesis that the selectivity switch can be attributed to the increase in hydroxide and, consequently, decrease in hydronium. The silver catalyst was also tested under nitrogen streams to eliminate product selectivity switch due to non-CO_2 reduction reactions, such as the reduction of $KHCO_3$ produced from the reaction of CO_2 with KOH. Using $KHCO_3$ as the electrolyte under nitrogen, hydrogen was the only product observed, indicating that the formate is a product of CO_2RR (Figure S6). To eliminate the potential effect, we ran the experiments at different current densities (25, 150, 300, and 450 mA/cm^2) within a wide potential range. The change of the CO and formate FEs within this potential range was around 5% (Figure S7), indicating that the switch in product selectivity is not due to the potential change. Our material characterizations show that silver is very stable under the reaction conditions and no change in bulk or surface was observed, indicating that the product selectivity is not due to catalyst change (Figures S8−10). Given these control experiments, we conclude that hydronium is the source of the selectivity switch between CO and formate, rather than material phase/voltage change[12] or cocatalytic chemisorption[13] effects.

Experimentally, under highly alkaline electrolytes ([KOH] > 1 M), negligible hydrogen evolution occurred, with the main competition for electrons being between CO and formate. In previous works[7d,14] using an H-Cell configuration, however, low CO_2 concentrations under higher pH conditions led to an increase in H_2 selectivity and dramatically decreased CO current densities, rather than an increase in formate production. Here the gas diffusion electrode and thin catalyst layer provide a sufficient supply of CO_2, not only preventing the hydrogen evolution reaction (HER), but allowing for the CO/formate

DOI: 10.1021/jacs.7b13542
J. Am. Chem. Soc. XXXX, XXX, XXX−XXX

selectivity switch phenomena to be experimentally observed. Therefore, the alkaline electrolyte not only suppresses HER, as claimed elsewhere,[7c,15] but must also alter the CO reaction pathway.

The bottom panel in Figure 3 further shows that a dramatic decrease of hydronium concentration to below 10^{-15} M leads to a sharp increase in the formate:CO ratio. However, it seems that even this small concentration of hydronium is enough to produce a significant amount of CO (ca. 40% FE). This may be due to either the significant effect of a trace amount of hydronium in stabilizing O−H bond formation within the COOH intermediate, or the existence of other parallel mechanisms for CO production (details provided in Supporting Information).

In summary, using DFT computations and experimental investigations, we studied the competing pathways of CO and formate on silver catalysts. Our theoretical studies highlighted the role of hydronium in the system as a driving factor determining reaction pathways and product selectivity. In the presence of hydronium, the CO pathway became more energetically favorable, as observed in many previous experimental studies. However, when hydronium was removed from the system, the activation energy barrier for formate was much lower than that of CO. Our experimental studies, where the amount of hydronium in the system was controlled using highly alkaline conditions, supported these theoretical predictions. The hydronium concentration was diminished sufficiently enough to switch the dominant product from CO to formate, producing almost 60% formate at 11 M KOH. We posit that using other electrolytes with controlled hydronium concentrations may lead to similar product selectivity switching. Though this work on silver demonstrates the function of hydronium on the CO_2RR pathway and, ultimately, its role on product selectivity, we postulate further investigations into the role of hydronium on other catalysts may open new theoretical and experimental routes to other product pathways.

■ ASSOCIATED CONTENT

Supporting Information

The Supporting Information is available free of charge on the ACS Publications website at DOI: 10.1021/jacs.7b13542.

Computational and experimental details (PDF)

■ AUTHOR INFORMATION

Corresponding Author

*ted.sargent@utoronto.ca

ORCID

Ali Seifitokaldani: 0000-0002-7169-1537
Christine M. Gabardo: 0000-0002-9456-6894
Thomas Burdyny: 0000-0001-8057-9558
Shana O. Kelley: 0000-0003-3360-5359
David Sinton: 0000-0003-2714-6408
Edward H. Sargent: 0000-0003-0396-6495

Author Contributions

⊥These authors contributed equally.

Notes

The authors declare no competing financial interest.

■ ACKNOWLEDGMENTS

The authors acknowledge support from the Natural Sciences and Engineering Research Council (NSERC) and the Government of Ontario through the Ontario Research Fund−Research Excellence program. All DFT computations were performed on the IBM BlueGene/Q supercomputer with support from the Southern Ontario Smart Computing Innovation Platform (SOSCIP). SOSCIP is funded by the Federal Economic Development Agency of Southern Ontario, the Province of Ontario, IBM Canada Ltd., Ontario Centres of Excellence, Mitacs and 15 Ontario academic member institutions. X-ray spectroscopy measurements were performed at the Canadian Light Source. A.S. thanks FRQNT for support in the form of postdoctoral fellowship award. C.M.G. thanks NSERC for support in the form of a postdoctoral fellowship award. T.B. thanks Hatch for a Graduate Scholarship for Sustainable Energy Research. J.P.E thanks NSERC, Hatch and the Government of Ontario for their support through graduate scholarships. M.K. acknowledges Banting postdoctoral fellowship from Government of Canada.

■ REFERENCES

(1) (a) Qiao, J.; Liu, Y.; Hong, F.; Zhang, J. *Chem. Soc. Rev.* **2014**, *43*, 631−675. (b) Jones, J.-P.; Prakash, G. K. S.; Olah, G. A. *Isr. J. Chem.* **2014**, *54*, 1451−1466.

(2) (a) Zheng, X.; De Luna, P.; García de Arquer, F. P.; Zhang, B.; Becknell, N.; Ross, M. B.; Li, Y.; Banis, M. N.; Li, Y.; Liu, M.; Voznyy, O.; Dinh, C. T.; Zhuang, T.; Stadler, P.; Cui, Y.; Du, X.; Yang, P.; Sargent, E. H. *Joule* **2017**, *1*, 794−805. (b) Innocent, B.; Liaigre, D.; Pasquier, D.; Ropital, F.; Léger, J.-M.; Kokoh, K. B. *J. Appl. Electrochem.* **2009**, *39*, 227. (c) Zhang, S.; Kang, P.; Meyer, T. J. *J. Am. Chem. Soc.* **2014**, *136*, 1734−1737. (d) Hara, K.; Kudo, A.; Sakata, T. *J. Electroanal. Chem.* **1995**, *391*, 141−147. (e) Hori, Y.; Wakebe, H.; Tsukamoto, T.; Koga, O. *Electrochim. Acta* **1994**, *39*, 1833−1839.

(3) (a) Saberi Safaei, T.; Mepham, A.; Zheng, X.; Pang, Y.; Dinh, C.-T.; Liu, M.; Sinton, D.; Kelley, S. O.; Sargent, E. H. *Nano Lett.* **2016**, *16*, 7224−7228. (b) Liu, M.; Pang, Y.; Zhang, B.; De Luna, P.; Voznyy, O.; Xu, J.; Zheng, X.; Dinh, C. T.; Fan, F.; Cao, C.; de Arquer, F. P. G.; Safaei, T. S.; Mepham, A.; Klinkova, A.; Kumacheva, E.; Filleter, T.; Sinton, D.; Kelley, S. O.; Sargent, E. H. *Nature* **2016**, *537*, 382. (c) Kim, C.; Jeon, H. S.; Eom, T.; Jee, M. S.; Kim, H.; Friend, C. M.; Min, B. K.; Hwang, Y. J. *J. Am. Chem. Soc.* **2015**, *137*, 13844−13850.

(4) (a) Yoshio, H.; Katsuhei, K.; Akira, M.; Shin, S. *Chem. Lett.* **1986**, *15*, 897−898. (b) Kuhl, K. P.; Hatsukade, T.; Cave, E. R.; Abram, D. N.; Kibsgaard, J.; Jaramillo, T. F. *J. Am. Chem. Soc.* **2014**, *136*, 14107−14113. (c) Pang, Y.; Burdyny, T.; Dinh, C.-T.; Kibria, M. G.; Fan, J. Z.; Liu, M.; Sargent, E. H.; Sinton, D. *Green Chem.* **2017**, *19*, 4023−4030.

(5) Hernandez, S.; Amin Farkhondehfal, M.; Sastre, F.; Makkee, M.; Saracco, G.; Russo, N. *Green Chem.* **2017**, *19*, 2326−2346.

(6) (a) Delacourt, C.; Ridgway, P. L.; Kerr, J. B.; Newman, J. *J. Electrochem. Soc.* **2008**, *155*, B42−B49. (b) Dufek, E.; Lister, T.; McIlwain, M. *J. Appl. Electrochem.* **2011**, *41*, 623−631. (c) Verma, S.; Lu, X.; Ma, S.; Masel, R. I.; Kenis, P. J. A. *Phys. Chem. Chem. Phys.* **2016**, *18*, 7075−7084.

(7) (a) Shi, C.; Chan, K.; Yoo, J. S.; Nørskov, J. K. *Org. Process Res. Dev.* **2016**, *20*, 1424−1430. (b) Montoya, J. H.; Shi, C.; Chan, K.; Nørskov, J. K. *J. Phys. Chem. Lett.* **2015**, *6*, 2032−2037. (c) Cheng, T.; Xiao, H.; Goddard, W. A. *J. Am. Chem. Soc.* **2016**, *138*, 13802−13805. (d) Singh, M. R.; Goodpaster, J. D.; Weber, A. Z.; Head-Gordon, M.; Bell, A. T. *Proc. Natl. Acad. Sci. U. S. A.* **2017**, *114*, E8812−E8821.

(8) (a) Chen, L. D.; Urushihara, M.; Chan, K.; Nørskov, J. K. *ACS Catal.* **2016**, *6*, 7133−7139. (b) Rosen, J.; Hutchings, G. S.; Lu, Q.; Rivera, S.; Zhou, Y.; Vlachos, D. G.; Jiao, F. *ACS Catal.* **2015**, *5*, 4293−4299.

(9) (a) Kim, B.; Ma, S.; Molly Jhong, H.-R.; Kenis, P. J. A. *Electrochim. Acta* **2015**, *166*, 271−276. (b) Hara, K.; Sakata, T. *Bull. Chem. Soc. Jpn.* **1997**, *70*, 571−576. (c) Thorson, M. R.; Siil, K. I.; Kenis, P. J. A. *J. Electrochem. Soc.* **2013**, *160*, F69−F74.

(10) Henkelman, G.; Jónsson, H. *J. Chem. Phys.* **2000**, *113*, 9978−9985.

DOI: 10.1021/jacs.7b13542
J. Am. Chem. Soc. XXXX, XXX, XXX−XXX

(11) (a) Nie, X.; Luo, W.; Janik, M. J.; Asthagiri, A. *J. Catal.* **2014**, *312*, 108−122. (b) Nie, X.; Esopi, M. R.; Janik, M. J.; Asthagiri, A. *Angew. Chem., Int. Ed.* **2013**, *52*, 2459−2462.
(12) Gao, D.; Zhou, H.; Cai, F.; Wang, D.; Hu, Y.; Jiang, B.; Cai, W.-B.; Chen, X.; Si, R.; Yang, F.; Miao, S.; Wang, J.; Wang, G.; Bao, X. *Nano Res.* **2017**, *10*, 2181−2191.
(13) Hollingsworth, N.; Taylor, S. F. R.; Galante, M. T.; Jacquemin, J.; Longo, C.; Holt, K. B.; de Leeuw, N. H.; Hardacre, C. *Angew. Chem., Int. Ed.* **2015**, *54*, 14164−14168.
(14) Hatsukade, T.; Kuhl, K. P.; Cave, E. R.; Abram, D. N.; Jaramillo, T. F. *Phys. Chem. Chem. Phys.* **2014**, *16*, 13814−13819.
(15) (a) Gao, D.; Wang, J.; Wu, H.; Jiang, X.; Miao, S.; Wang, G.; Bao, X. *Electrochem. Commun.* **2015**, *55*, 1−5. (b) Wu, J.; Risalvato, F. G.; Ke, F.-S.; Pellechia, P. J.; Zhou, X.-D. *J. Electrochem. Soc.* **2012**, *159*, F353−F359.

DOI: 10.1021/jacs.7b13542
J. Am. Chem. Soc. XXXX, XXX, XXX−XXX